ISSN 0031-918X, The Physics of Metals and Metallography, 2013, Vol. 114, No. 6, pp. 529–534. © Pleiades Publishing, Ltd., 2013.
Original Russian Text © O.G. Khadzhieva, A.G. Illarionov, A.A. Popov, S.V. Grib, 2013, published in Fizika Metallov i Metallovedenie, 2013, Vol. 114, No. 6, pp. 577–582.

STRUCTURE, PHASE TRANSFORMATIONS, AND DIFFUSION

Effect of Hydrogen on the Structure of Quenched Orthorhombic Titanium Aluminide-Based Alloy and Phase Transformations during Subsequent Heating

O. G. Khadzhieva, A. G. Illarionov, A. A. Popov, and S. V. Grib

The First President of Russia B. N. Yeltsin Ural Federal University, ul. Mira 19, Ekaterinburg, 620002 Russia
e-mail: illarionovag@mail.ru; olga.khadzhieva@gmail.com

Received November 13, 2012

Abstract—The effect of hydrogen on structure formation and changes in the volume fractions of phases in an alloy based on orthorhombic titanium aluminide (*O* phase) alloy upon its quenching is studied. X-ray diffraction analysis is used to determine the lattice parameters of phases. It has been shown that hydrogen is dissolved mainly in the β_0 phase. Differential thermal analysis is used to determine stages and temperature ranges of phase transformations during heating; it was found that introduced hydrogen shifts the $\beta_0 \rightarrow O$ and reverse $O \rightarrow \beta_0$ transformations into the low-temperature range; the enthalpies of transformation are calculated.

Keywords: hydrogen, *O* phase, titanium aluminides, heating, phase transformations, titanium alloys
DOI: 10.1134/S0031918X13060070

INTRODUCTION

Interest of investigators to titanium intermetallic-based alloys is related to their high-performance high-temperature strength and heat resistance. These alloys exceed industrial high-temperature titanium alloys in these characteristics and can compete with steels and nickel alloys at operating temperatures of to 700–750°C [1]. Alloys based on orthorhombic titanium aluminide Ti_2AlNb (*O* phase) [1] are the most manufacturable and show promise for aerospace engineering applications. However, the preparation of deformed half-finished products from these alloys is difficult. Studies performed at the Tsiolkovskii Moscow State Aviation Technological University showed hydrogen-induced plasticity effects, which were found to be useful in improving the production technology of half-finished products and articles made from hardly deformed titanium alloys [2, 3], which includes hydrogen heat treatment (HHT) [4–6]. Previously, we considered the effect of hydrogen on the formation of phase composition and structure of Ti_2AlNb-base alloy during quenching from different temperatures [7]. It was shown that the hydrogen incorporation suppresses the formation of α_2 phase in this alloy and decreases temperatures of transformation into the single-phase β and disordered ($B2 \rightarrow A2$ transition) states during heating. However, up to now, problems related to the effect of hydrogen alloying on the occurrence of phase transformations in quenched alloys during heating remains poorly understood.

The aim of the present study is to investigate the effect of hydrogen alloying on the formation of the phase composition and structure of quenched *O*-phase-based alloy and occurrence of transformations during subsequent continuous heating.

EXPERIMENTAL

Cylindrical samples 20 mm in diameter, which were turned from the central portion of a titanium alloy ingot, were used as the material for the investigation. The chemical composition of the alloy (at %) is Ti–24.3 Al–24.8 Nb–0.1 Zr–0.6 Mo–0.3 Si [7] and corresponds to the Ti_2AlNb-based intermetallics (*O* phase). The samples were hydrogenated at 900°C using gaseous hydrogen at a pressure of to 80 kPa and using a Sieverts-type apparatus.[1] The hydrogen content reached in the samples is 5.2 at %. The samples were marked as follows: the hydrogen-free alloy is Alloy 1 and the sample with 5.2 at % H is Alloy 2.

The samples of Alloys 1 and 2 were subjected to water quenching from a temperature of 900°C. The choice of the quenching temperature was due to data available in [7]. It was shown in [7] that, at this temperature, first, no grain growth takes place in the β phase and, second, the amount of the β phase capable of decomposition during subsequent aging is significant (50 and 70% in Alloys 1 and 2, respectively).

[1] The hydrogen-free and hydrogenated samples were kindly supplied by Prof. G.A. Salishev in terms of cooperation.

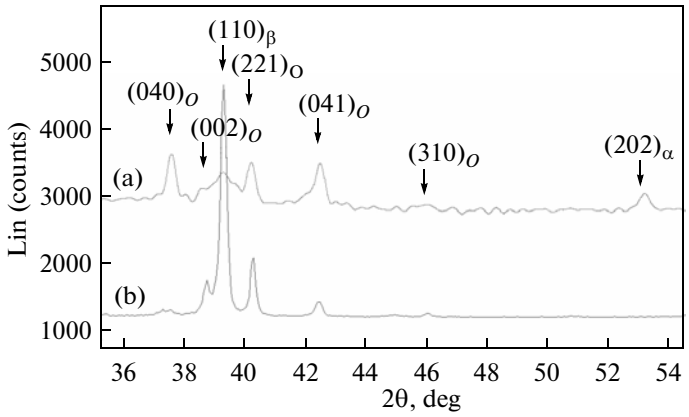

Fig. 1. X-ray diffraction patterns of quenched alloys: (a) Alloy 1 and (b) Alloy 2.

The microstructure of alloys was studied by scanning electron microscopy (SEM) using a Philips 535 microscope and an accelerating voltage of 30 kV.

X-ray diffraction (XRD) analysis was performed using a Bruker D8 Advance diffractometer, Cu $K\alpha$ radiation, energy dispersion detector, and Soller gaps. X-ray patterns were taken by scanning in an angular range $2\theta = 20°–85°$ at a step of 0.05°; the time per step is 3 s. The XRD data were used to calculate the lattice parameters of β_0- and *O*-phases. The $(400)_O$ reflection was used to determine the lattice parameter *a*; the $(040)_O$ and $(310)_O$ reflections were used to determine the lattice parameter *b*. The lattice parameter *c* was calculated using the $(043)_O$ and $(042)_O$ reflections.

Temperature ranges of phase transformations in the quenched alloys were determined during heating using simultaneous thermal analysis (STA), which includes the differential scanning calorimetry (DSC) and thermal gravimetric analysis (TGA). Samples were heated to 1200°C at a rate of 20 K/min in a protective argon atmosphere using a STA 449 C Jupiter cell. The error of the temperature determination is ±2°C.

RESULTS AND DISCUSSION

Effect of Hydrogen on Formation of Phase Composition and Structure of Alloy during Quenching

According to XRD data, the three-phase state ($O + \beta_0$ and α_2) is fixed in Alloy 1 during its quenching (Fig. 1a). It should be noted that the β solid solution is ordered with the formation of the *B*2 structure (in the text, it is called β_0). As was shown in [7], the hydrogen introduction suppresses the formation of the α_2 phase during quenching; this results in the formation of a two-phase ($O + \beta_0$) structure (Fig. 1b).

Variations in lattice parameters of quenched alloys

	Lattice parameter of β_0 phase, $\times 10^{-1}$ nm	Lattice parameters of *O* phase, $\times 10^{-1}$ nm		
	a_β	a_O	b_O	c_O
Alloy 1	0.3254	0.6048	0.9583	0.4656
Alloy 2	0.3278	0.6055	0.9650	0.4662

The microstructure of the quenched alloys is shown in Fig. 2.

It can be seen from Fig. 2 that, after the quenching of Alloy 1, significant amounts of α_2- and *O*-phase plates are fixed in the β_0 matrix. According to the data of the earlier study [7], the larger plates are the α_2 phase; *O*-phase plates are smaller and located between α_2-phase plates. The matrix β_0 phase is observed in the form of thin layers between plates (Fig. 2a). The presence of hydrogen in Alloy 2 leads to the coarsening of *O*-phase plates and the retention of a higher volume fraction of the β_0 matrix phase in the structure than in Alloy 1 (Fig. 2b).

The lattice parameters of the β_0 and *O* phases were calculated using XRD data (see table). An analysis of the results obtained shows that the hydrogen introduction leads to an increase in the lattice parameter of the β_0 phase. It is known [2] that hydrogen is dissolved mainly in the β phase and favors the swelling of its lattice. It was also shown in [8] that the analogous tendency toward the increase in the lattice parameter a_β is observed for hydrogen-alloyed Ti–Al–Nb compositions with lower Nb contents.

The effect of hydrogen on the lattice parameters of *O* phase was analyzed. It was found that no significant changes in the lattice parameter *c* of the *O* phase are observed for hydrogen-containing alloys; the lattice parameters *a* and *b* increase. However, this does not change the rhombicity of the lattice; the *b*/*a* ratio remains almost unchanged and, for Alloys 1 and 2, equals 1.585 and 1.593, respectively. It was shown in [8] that, for intermetallic Ti–Al–Nb compositions with 10 at % Nb and up to 11 at % H, the hydrogenation leads to an increase in the lattice parameter *a* of the *O* phase; in this case, the lattice parameter *b* decreases. This leads to a decrease in the *b*/*a* ratio from 1.732 to 1.640; similar to our case, the lattice

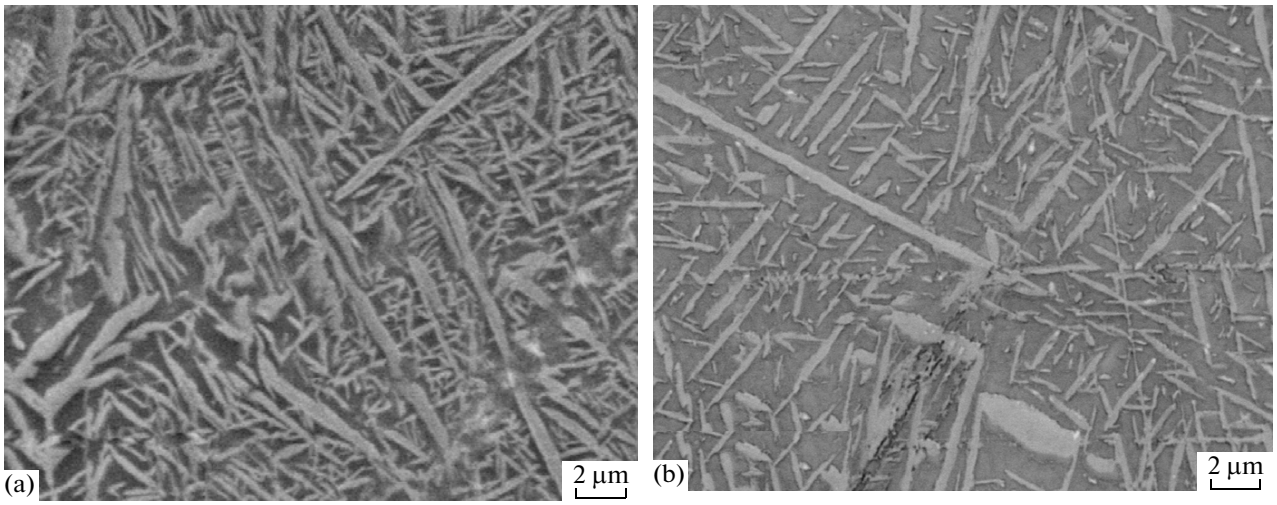

Fig. 2. Microstructure of alloys after quenching from 900°C: (a) Alloy 1 and (b) Alloy 2.

parameter *c* is unchanged and equals about 0.4656. In a number of studies [8, 9], the *O*-phase lattice is considered to be pseudo-hexagonal and characterized by distortions due to the supersaturation with Nb. Authors of study [10] assume that hydrogen atoms occupy octapores in the hcp lattice of titanium, since they are larger in size than tetra-pores, which is sufficient for the location of a hydrogen atom. In this study, different kinds of octapores present in the hcp lattice of the Ti_3Al intermetallic are considered (these include two octapores formed by Ti atoms (first kind) and six octapores formed by Ti and Al atoms (second kind)) and it is shown that, when assuming the minimum free energy of hydrogen solution in the Ti_3Al intermetallic, hydrogen atoms primarily occupy octapores formed by Ti atoms. When the orthorhombic lattice of the *O* phase is considered as pseudohexagonal, 16 slightly distorted octapores are present. Among them, eight pores are formed by 4 Ti atoms, 1 Al atom, and 1 Nb atom; four pores are formed by 2 Ti atoms, 1 Al atom, and 3 Nb atoms; and four pores are formed by 2 Ti atoms, 3 Al atoms, and 1 Nb atom. In this case, one may assume that hydrogen atoms occupy mainly first-kind octapores formed by maximum number of Ti atoms. These pores are located along the [010] and [100] directions and result in the observed increase in the lattice parameters *a* and *b* and unchanged lattice parameter *c*.

The lattice parameters of the *O* and β phases were used to calculate unit-cell volumes per atom for quenched alloys with different hydrogen contents (Fig. 3).

The histogram (Fig. 3) demonstrates that the hydrogen-induced increase in the unit-cell volume per atom of the β_0 phase (~2%) is higher than that for the *O* phase (to 1%). This is likely related to the higher hydrogen solubility in the β_0 phase. The data given in Fig. 3 were used for calculations, which showed that the unit-cell volume per atom for the β_0 phase in Alloy 1 is 2% higher than that for the *O* phase (the analogous data were obtained in [11, 12]); the hydrogen introduction (Alloy 2) increases the difference to 3.5%.

Effect of Hydrogen on the Occurrence of Transformations in Quenched Alloys during Continuous Heating

Figure 4 shows a DSC curve measured for Alloy 1 during continuous heating. Four thermal effects are observed in the curve; these include the exothermic effect observed in the temperature range of 700–875°C (the temperature of peak is 765°C) and four endothermic effects that correspond to temperature ranges of 877–1017°C (the temperature of minimum is 951°C), 1020–1070°C (the temperature of minimum is ~1040°C), and 1140–1170°C (the temperature of minimum is 1150°C).

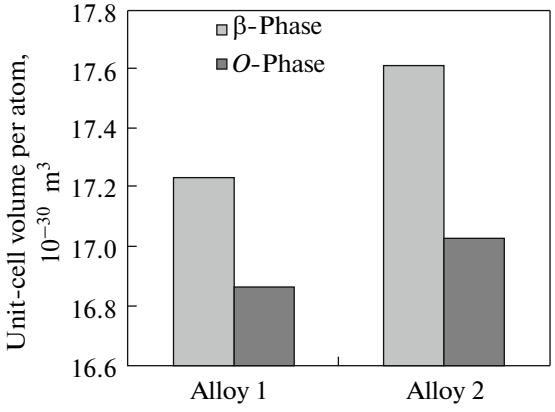

Fig. 3. Changes in the unit-cell volume per atom for the phases.

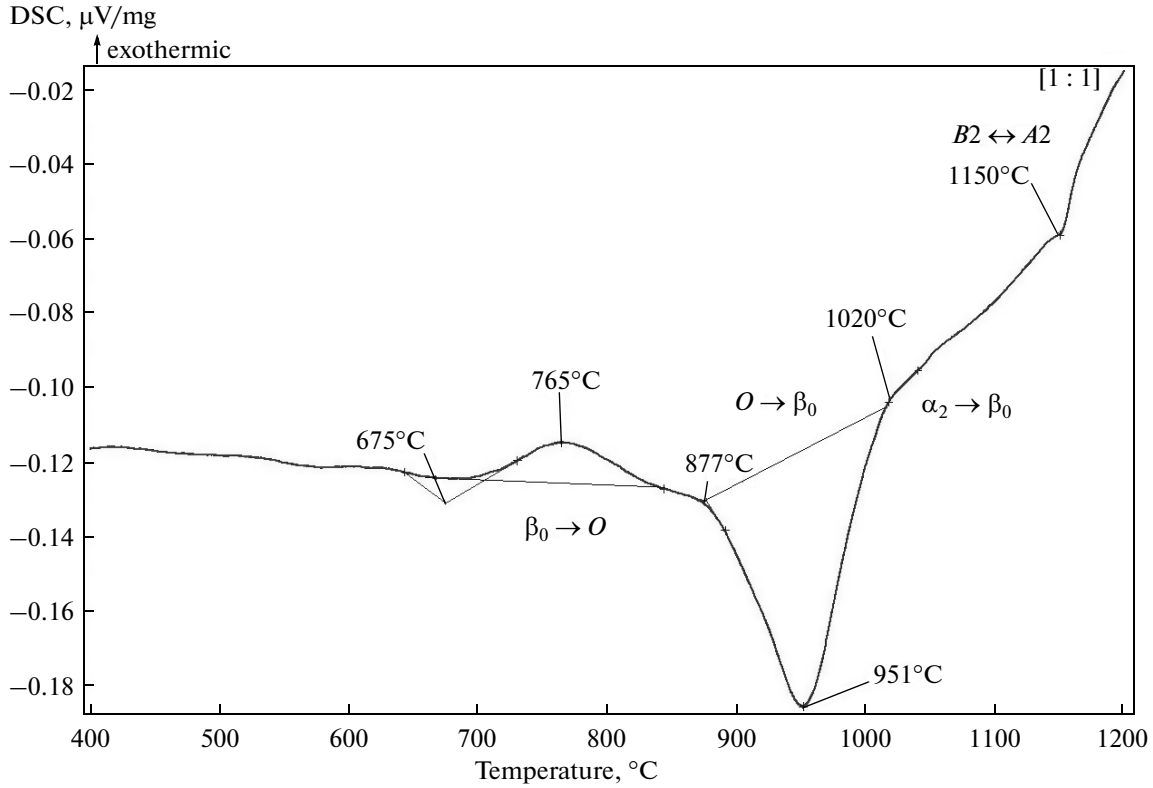

Fig. 4. DSC curve measured for Alloy 1 during continuous heating.

A comparison of the data with the phase diagram [13] and data of [7] allows us to conclude that the exothermic effect is related to the occurrence of the $\beta_0 \rightarrow O$ transformation (decomposition of a metastable solid solution fixed during quenching), which is accompanied by the precipitation of the O phase. The first endothermic effect corresponds to the realization of reverse $O \rightarrow \beta_0$ transformation (dissolution of the O phase); the second endothermic effect is related to the $\alpha_2 \rightarrow \beta_0$ transformation (dissolution of the α_2 phase). The found temperature ranges of phase transformations agree adequately with data of [13, 14]. Within the temperature range of the third effect, an order–disorder transition takes place; in this case, the ordered β_0 phase with the $B2$ structure transforms into a disordered phase with the bcc $A2$ structure (the transformation $B2 \leftrightarrow A2$ is shown in the DSC curve). This transition was found at close temperatures in [12, 15].

Figure 5 shows the DSC curve measured for Alloy 2 during heating.

A comparison of the DSC curve for Alloy 2 with that for Alloy 1 allows us to note a number of distinctive peculiarities. First, the intensity of exothermic effect related to the $\beta_0 \rightarrow O$ transformation increases substantially; the peak shifts to the low-temperature range. Second, within the temperature range that corresponds to the reverse $O \rightarrow \beta_0$ transformation, an asymmetric endothermic effect with an inflexion is observed just near the quenching temperature (900°C). In our opinion, the observed asymmetry is related to the dissolution of the O phase of two different kinds. First, the O phase formed upon the $\beta_0 \rightarrow O$ transformation during continuous heating of quenched alloy is dissolved; after that, the O phase formed during heating before quenching is dissolved. The analogous asymmetry of the endothermic effect near the quenching temperature was found for the $\alpha \rightarrow \beta$ transformation in a high-alloyed titanium alloy preliminarily quenched from the two-phase region [16]. Moreover, similar to the effect related to the $\beta_0 \rightarrow O$ transformation, the considered endothermic effect also shifts to the low-temperature range; the temperatures of minimum and nominal end of transformation is 925 and 993°C, respectively. Third, the endothermic effect related to the $\alpha_2 \rightarrow \beta_0$ transformation disappears likely because of the earlier-found [7] hydrogen-suppressed formation of α_2 phase in the alloy. Fourth, as compared to the endothermic effect related to the disordering of Alloy 1, the effect in the hydrogen-containing alloy shifts to the lower-temperature range (temperature of minimum is 1130°C).

The area under the curve of the exothermic effect, that corresponds to the $\beta_0 \rightarrow O$ transformation, was used to calculate the enthalpy of the transformation. The calculations showed that the magnitudes for

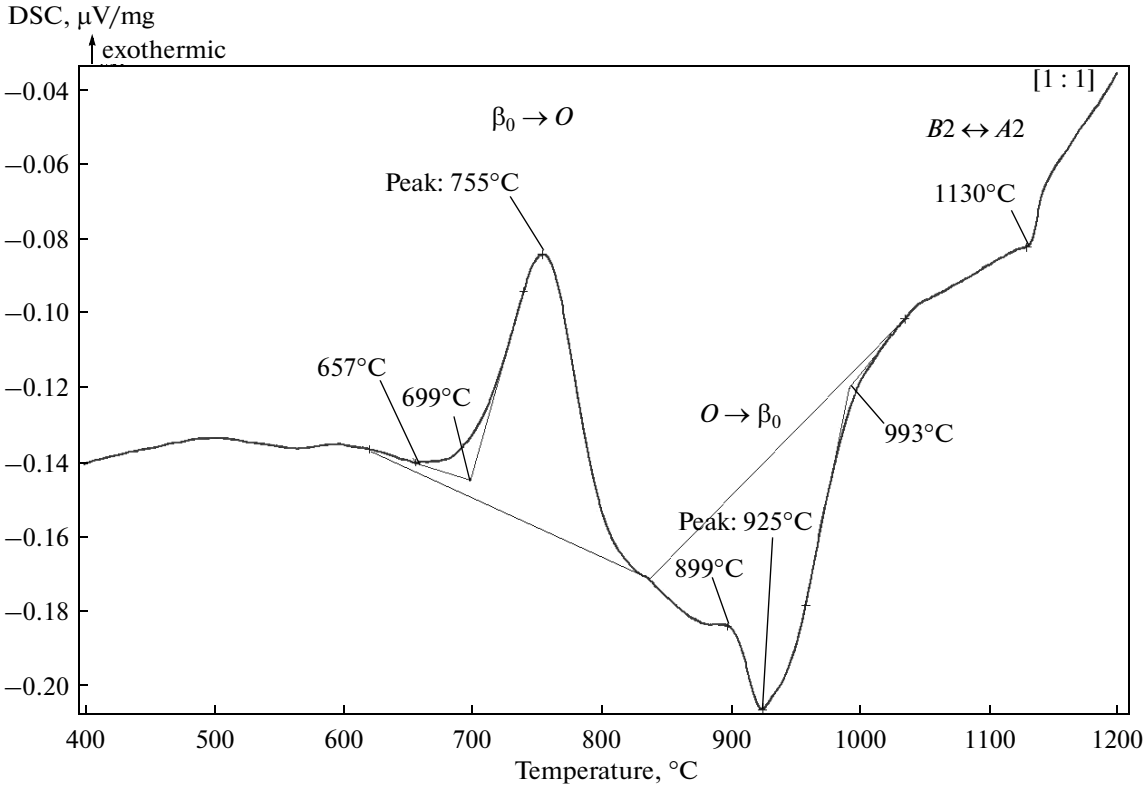

Fig. 5. DSC curve measured for Alloy 2 during continuous heating.

Alloys 1 and 2 are 4.83 and 23.96 J/g, respectively. The observed increase in enthalpy is related to the increase in the volume fraction of the β_0 phase, which is fixed upon quenching and capable of decomposing during the heating of the hydrogen-containing alloy.

CONCLUSIONS

(1) It was shown that, after hydrogen introduction, the rhombicity of the *O*-phase lattice in the quenched alloy is almost unchanged; the lattice parameter ratio *b*/*a* is 1.584 and 1.593 for the hydrogen free alloy (Alloy 1) and Alloy 2, respectively. The lattice parameter *c* is 0.4656 nm and remained unchanged for all hydrogen concentrations. This is likely related to the ordered arrangement of hydrogen atoms in the *O*-phase lattice.

(2) The unit-cell volumes per atom for the β_0 and *O* phases were calculated. The quenched alloys with different hydrogen contents were found to exhibit a more substantial increase in the β_0-phase unit-cell volume per atom as compared to the *O*-phase unit-cell volume due to the higher solubility of hydrogen in the β_0 phase.

(3) The hydrogen-induced increase in the difference between the specific unit-cell volumes of the β_0 and *O* phases is to 3.5%. This can favor the phase recrystallization and, therefore, opens up possibilities for controlling the structure of the alloy under study by heat treatment.

(4) The stages and temperatures ranges of phase transformations that occurred during the continuous heating of the alloys were found. It is shown that the hydrogen introduction shifts the $\beta_0 \rightarrow O$ and reverse $O \rightarrow \beta_0$ transformation to the lower-temperature range as compared to that for the hydrogen-free alloy. The enthalpy of the $\beta_0 \rightarrow O$ phase transformation for alloys 1 and 2, was calculated to be 4.83 and 23.96.

ACKNOWLEDGMENTS

In the present study, we use results obtained with the equipment available in the laboratory for Structural Methods of Analysis and Properties of Materials and Nanomaterials at the Center of Collaborative Access, Ural Federal University.

REFERENCES

1. A. A. Il'in, B. A. Kolachev, and I. S. Pol'kin, *Titanium Alloys: Composition, Structure, Properties* (VILS-MATI, Moscow, 2009) [in Russian].
2. A. A. Il'in, B. A. Kolachev, V. K. Nosov, and A. M. Mamonov, *Hydrogen Technology of Titanium Alloys* (MISIS, Moscow, 2002) [in Russian].

3. V. K. Nosov and B. A. Kolachev, *Hydrogen Plastification upon Hot Deformation of Titanium Alloys* (Metallurgiya, Moscow, 1986) [in Russian].
4. V. K. Nosov, A. A. Il'in, V. N. Uvarov, et al., "Hydrogen plastification and thermohydrogen treatment upon the production of semifinished products from Ti_3Al-based alloys," *Proc. Ist Int. Conf. on Titanium of the Commonwealth Independent States "Science, Production and Application of Titanium in Conversion Conditions," Moscow, 1994*, pp. 668–674.
5. A. A. Il'in, A. M. Mamonov, and V. K. Nosov, "Scientific foundations and principles of formation of technological processes of thermohydrogen treatment of titanium alloys," Izv. Ross. Akad. Nauk, Ser. Met., No. 4, 157–168 (1994).
6. A. A. Il'in, A. M. Mamonov, V. V. Zasypkin, and O. A. Bytsenko, "Formation of bimodal structure and optimization of mechanical properties of heat-resistant intermetallic Compound Ti_3Al-based alloy by thermohydrogen treatment," Titan, No. 2, 45–50 (2004).
7. A. G. Illarionov, S. V. Grib, A. A. Popov, S. L. Demakov, M. S. Karabanalov, O. G. Khadzhieva, and O. A. Elkina, "Effect of hydrogen on the formation of the structure and phase composition in the Ti_2AlNb-based alloy," Phys. Met. Metallogr. **109**, 142–152 (2010).
8. X. Pierron, M. de Graef, and A. W. Thompson, "On the effect of hydrogen on the microstructure of α_2-Ti_3Al + Nb alloys," Philos. Mag. A **77**, 1399–1421 (1998).
9. W. Ying, Y.. de Zhuang, and M. Gui, "The formation mechanism of the O phase in a Ti_3Al–Nb Alloy," Intermetallics **8**, 629–632 (2000).
10. S. P. Belov, A. A. Il'in, A. M. Mamonov, and A. V. Aleksandrova, "Theoretical analysis of the ordering processes in Ti_3Al-based alloy: Effect of hydrogen on Ti_3Al intermetalic compound stability," Izv. Ross. Akad. Nauk, Ser. Met., No. 2, 76–80 (1994).
11. A. A. Popov, A. G. Illarionov, S. V. Grib, S. L. Demakov, M. S. Karabanalov, and O. A. Elkina, "Phase and structural transformations in the alloy on the basis of the orthorhombic titanium aluminide," Phys. Met.Metallogr. **106**, 399–410 (2008).
12. F. A. Sadi and C. Servant, "On the $B2 \rightarrow O$ phase transformation in Ti–Al–Nb alloys," Mater. Sci. Eng., A **346**, 19–28 (2003).
13. C. J. Boehlert, B. S. Majumdar, V. Seetharaman, and D. B. Miracle, "Part I. The microstructural evolution in Ti–Al–NbO+BCC orthorhombic alloys," Metal. Mater. Trans. A **30**, 2305–2323 (1999).
14. A. K. Gogia, T. K. Nandy, D. Banerjee, T. Carisey, J. L. Strudel, and J. M. Franchet, "Microstructure and mechanical properties of orthorhombic alloys in the Ti–Al–Nb System," Intermetallics **6**, 741–748 (1998).
15. V. Chaumat, E. Ressouche, B. Ouladdiaf, P. Desre, and F. Moret, "Experimental study of phase equilibria in the Nb–Ti–Al system," Scr. Metall. **40**, 905–911 (1999).
16. A. G. Illarionov, S. L. Demakov, A. A. Popov, I. V. Medvedeva, M. S. Karabanalov, and O. A. Elkina, "Structural phase transformations in (α + β) titanium alloy of Ti–10V–2Fe–3Al transition class at hardening thermal treatment," Titan, No. 3, 27–33 (2009).

Translated by N. Kolchugina